Hybrid Space-Ground Processing for High-Capacity Multi-beam Satellite Systems

J. Arnau-Yañez[§], M. Bergmann[†], E.A. Candreva[*], G.E. Corazza[*], R. de Gaudenzi [¶], B. Devillers[‡], W. Gappmair[†], F. Lombardo[*], C. Mosquera[§], A. Pérez-Neira[‡], I. Thibault[*], A. Vanelli-Coralli[*]

[*]DEIS/ARCES University of Bologna,
viale del Risorgimento, 2, 40134 Bologna, Italy
email: {gecorazza, avanelli, ecandreva, ithibault, flombardo}@arces.unibo.it
[†]Institute of Communication Networks and Satellite Communications, Graz University of Technology
Inffeldgasse 12, 8010 Graz, Austria
email: {michael.bergmann, gappmair}@tugraz.at
[‡]Centre Tecnologic de Telecomunicacions de Catalunya (CTTC)
Parc Mediterrani de la Tecnologia (PMT), Av. Carl Friedrich Gauss 7, 08860 - Castelldefels, Barcelona, Spain
email: {aperez, bertrand.devillers}@cttc.es
[§] Signal Theory and Communications Department
University of Vigo - 36310 Vigo, Spain
email: {suso, mosquera}@gts.uvigo.es
[¶] RF Payload Systems Division, European Space Agency (ESA/ESTEC)
Keplerlaan 1, P.O. Box 299, AG Noordwijk, The Netherlands
email: riccardo.degaudenzi@esa.int

***Abstract*—Signal processing in satellite applications is usually performed either *on-ground* or *on-board*, i.e. at the gateway station or in the payload. Within the framework of the *European Space Agency* (ESA) SatNEx III study, a hybrid approach has been considered by splitting the processing between the satellite and the gateway, aiming to strike a better balance between performance and payload complexity. The design of a high-capacity multi-beam system has been carried out, to assess the potential applicability of a hybrid space-ground processing architecture (DIGISAT) for satellite broadband systems; this is achieved via hybrid space-ground beamforming, MIMO and MIMO-MUD, Precoding, as well as Digital Feeder link techniques.**

Keywords: Hybrid Space-Ground processing, Beamforming, MUD, MIMO, Precoding

I. INTRODUCTION

Signal processing techniques for Satellite applications can be classified as *on-ground*, *on-board* and *hybrid*. In the first two cases, the processing is performed by the gateway and the payload, respectively. The hybrid approach, on the other hand, consists in splitting the processing between the satellite and the gateway, aiming to some optimization of the trade-off between performance and payload complexity. Within the framework of the *European Space Agency* (ESA) SatNEx III (Satellite Network of Experts) study, the design of a high-capacity multi-beam system has been carried out, showing potential gains deriving from the use of joint Multi-User Detection (MUD) or Precoding, and Beamforming (BF) techniques.

More in detail, the study started with a system in which joint techniques were applied fully on ground, moving then to hybrid processing. The aim of hybrid solutions is to reduce the feed signal space to a subspace, by means of such a split processing, thus reducing feed capacity requirements; moreover, the digitization of the feeder link will represent a significant advantage with respect to present-day systems, since there will be no more need of calibration, as in analogue space-ground links, and compression techniques, joint with efficient coding and modulation schemes, will make the feeder link more efficient. A schematic representation of the considered hybrid architecture, named DIGISAT, is given in Fig. 1.

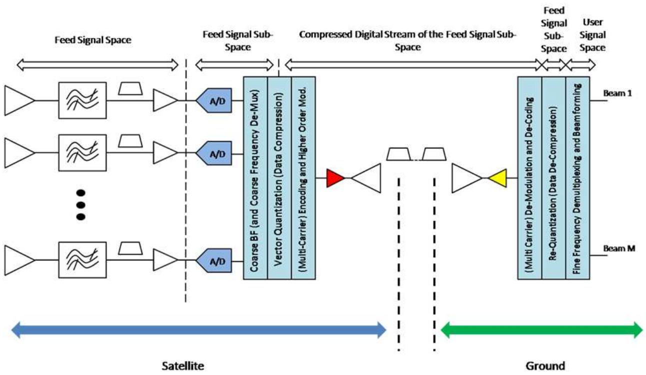

Fig. 1. Digisat architecture

This paper reports the outcomes of such an ambitious research effort, and it is organized as follows: after a brief description of the system model in Section II, channel estimation techniques for both the forward link (FL) and the return link (RL) are presented in Section III. Section IV and V deal with multi-user interference mitigation techniques, operating in both the feeds space and the beams space, for the FL (joint BF and linear precoding) and the RL (joint BF and MUD), respectively. Section VI describes the architecture of the digital feeder link and the hybrid BF approach, and some compression techniques are presented.

Notation: Boldface uppercase letters denote matrices and boldface lowercase letters refer to column vectors. We denote by $(.)^H$ the Hermitian transpose, and by $\mathbf{I}$ the identity matrix of adequate dimensions.

II. System Model

It is assumed that the forward and return links are related to $K = 100$ beams, pointing to 100 user cells, henceforth meant to serve 100 (UTs) simultaneously, i. e., a single UT per beam/cell at a given time. According to the antenna model provided by ESA, the beams are formed by an array of $N = 155$ feeds; Fig. 2 depicts the 3 dB contour plot of the feeds' radiation pattern on ground, each of them indicated by a separate number. Every beam integrates 20 feeds tuned appropriately in amplitude and phase so as to achieve the required beamforming.

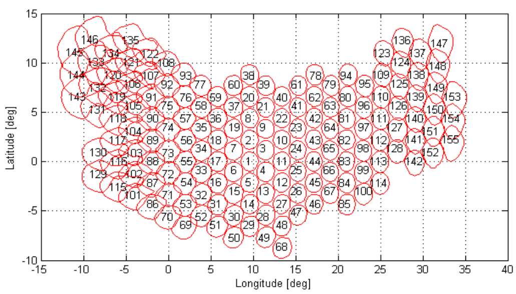

Fig. 2. Contour plot (3 dB) of the 155 satellite feeds.

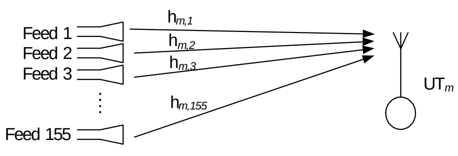

Fig. 3. Satellite downlink for the m-th user terminal.

First we consider the forward link (FL) of a broadband satellite system, where a gateway (GW) provides broadband service simultaneously to K UTs. Neglecting frequency selective effects and fast time-varying fading, we can model the forward link as

$$\mathbf{y} = \mathbf{H}\mathbf{x} + \mathbf{n} \tag{1}$$

where the $N \times 1$ vector $\mathbf{x}$ is the stack of the transmitted signals at all feeds, and $\mathbf{y}$ (resp. $\mathbf{n}$) is a $K \times 1$ vector containing the received signal (resp. noise) at the UTs. The $K \times N$ channel matrix is denoted by $\mathbf{H}$. More in detail, the m-th row of the channel matrix, i. e., $\mathbf{h}_m = (h_{m,1}, h_{m,2}, \ldots, h_{m,N})$, $m = 1, 2, \ldots, K$, includes $N = 155$ complex-valued numbers characterizing the connection between GW and the m-th UT, simply denoted by UT_m as sketched in Fig. 3. The channel matrix $\mathbf{H}$ accounts for the feed radiation pattern, the path loss, the atmospheric fading, the receive antenna gain, and the noise power (such that $\mathbf{E}\{\mathbf{n}\mathbf{n}^H\} = \mathbf{I}$). The constraint on the average power transmitted at the feed level is expressed as $\mathbf{E}[\mathbf{x}^H\mathbf{x}] \leq P$.

The same model can be applied to the return link, where rows and columns of the involved matrices are reflecting data transmission from UTs to the GW, thus the mathematical description of the K UT signals being received by the N on-board feeds is given by Eq. (1) as well, where $\mathbf{y}$ and $\mathbf{n}$ are $N \times 1$ vectors, $\mathbf{x}$ is a $K \times 1$ vector and $\mathbf{H}$ is the $N \times K$ channel matrix. In this case it is more convenient to operate a different normalization with respect to the forward link, and we will assume that $\mathbf{E}\{\mathbf{x}\mathbf{x}^H\} = \mathbf{I}$.

The practical setup considered in this paper is based on a $\mathrm{K_a}$ band foward link, operating at 20 GHz and having a total bandwidth of 500 MHz subdivided into 12 carriers in a single color freqency reuse scheme. The system is supposed to operate with the DVB-S2 standard, the operating points of which, for various modulation and coding schemes, have been taken as a reference. The return link has the same bandwidth, but operating at 30 GHz, and it is supposed to be based on the DVB-RCS2 standard (which will be soon released), so the baudrate is 4 Msymb/s and the guardbands amount to the 11% of the carrier bandwidth. Color schemes 3 and 1 were studied, corresponding to 166 and 500 MHz available bandwidth per beam, respectively.

Before dealing with a detailed evaluation of the key techniques of this system, a clarification on the scenario is in order. We are supposing that a single GW is in charge of the whole processing, and we are presenting the achievable gain in such a scenario. In present day systems, on the other hand, a GW can process just a cluster of around 10 beams rather than the total number of beams. This is due to the limitation in feeder link bandwidth, and this may result in a decrease of the potential gain offered by multi-user interference mitigation techniques.

III. Forward and Return Channel Estimation

In satellite communications, the multi-beam concept is closely related to a major problem: adjacent spots are affected by *interference*, in particular if operated at full frequency reuse [2]. In the DIGISAT context, this problem is to be mitigated by appropriately selected ground segment algorithms. Most promising in this respect are linear or nonlinear precoding schemes on the forward link and powerful interference cancellation techniques on the return link [3], [4]. But no matter which kind of mitigation method we are going to implement at the end, for proper operation the corresponding channel state

TABLE I
SIMULATION PARAMETERS

FL simulation parameters	
UTs location distribution	Uniformly distributed
UT antenna gain G_R^2	41.7dBi
UT clear sky $G_R^2/T_{ClearSky}$	17.68dB/K
UT rain delta temperature	221.83K
Atmospheric fading	City of Rome [1]
RL simulation parameters	
Training sequence length	1,000 symbols
Feed and beam gain patterns	Generated from data provided by ESA
Receiver noise figure	2.5 dB
Total receiver noise temperature	517 K
Fading	Rician, $K = 15$ dB
Atmospheric fading	City of Rome

information (CSI) has to be known by the gateway station so as to initialize precoding and cancellation algorithms.

Based on the system model reported in Section II, and focusing first on the forward link in the feed space, it is clear that the received signal at UT_m is given by

$$\mathbf{y}_m = \mathbf{h}_m \mathbf{C} + \mathbf{n}_m \tag{2}$$

where matrix $\mathbf{C}$ contains the complete set of N unique words (UWs) as row vectors of length L and $\mathbf{n}_m$ denotes the sequence of zero-mean white Gaussian noise samples.

The channel matrix must be known to the GW station for interference mitigation on both forward and return links. This might be achieved by a separate calibration network; a more elegant and less expensive solution for this purpose, however, is the usage of the communication network as such. In this context, the estimate of $\mathbf{h}_m$ is straightforwardly obtained by post-multiplying (2) with the *Moore-Penrose pseudo-inverse* of $\mathbf{C}$, i. e., $\mathbf{C}^+ = \mathbf{C}^{\mathrm{H}}(\mathbf{C}\mathbf{C}^{\mathrm{H}})^{-1}$. As a consequence, we arrive at

$$\hat{\mathbf{h}}_m = \mathbf{y}_m \mathbf{C}^+ = \mathbf{h}_m + \mathbf{e}_m \tag{3}$$

with the error vector evaluated as

$$\mathbf{e}_m = \mathbf{w}_m \mathbf{C}^+. \tag{4}$$

Basically, the FL model discussed so far can be applied for channel estimation in the beam space as well. The only difference is that channel and UW matrices have to be defined accordingly, and this holds also true for the return link.

A. Forward Link Analysis

Orthogonal sequences with $\mathbf{C}\mathbf{C}^{\mathrm{H}} = \mathbf{I}$ are best suited for FL estimation since they do not produce interference noise. Unfortunately, the frequently used Walsh-Hadamard (WH) codes are all of length $L = 2^n$, $n \in \mathbb{N}$. On the other hand, channel estimates achieved via *non-orthogonal* sequences of arbitrary length suffer from a significant error amplification if the related pseudo-inverse exists, or from a substantial jitter floor if $\mathbf{C}^+$ does not exist so that $\mathbf{C}^{\mathrm{H}}$ has to be used instead [5].

B. Return Link Analysis

In contrast to forward links, data transmission on return links can *not* be regarded as symbol-synchronous, which is mainly due to the different UT locations as well as the different propagation conditions between satellite and each terminal. But it can be assumed that the data rates on the RL are small enough so that the discrepancy will be only on the order of a few symbols; this is usually compensated by an appropriately chosen *guard time* between frames so that data transmission on RLs might be organized in a frame-synchronous manner. As a consequence, WH codes would not be optimal as their orthogonality gets lost in such an environment; instead, correlation with random sequences (one per link) with good cross-correlation properties are suggested for this purpose.

IV. MULTI-USER INTERFERENCE MITIGATION FOR THE FORWARD LINK

A. Linear Precoding for the Forward Link

We consider multi-user interference mitigation techniques in the FL in the form of linear precoding implemented on-ground at the GW. The following two scenarios are considered:

(i) Fixed beamforming and precoding [2]: assume a fixed on-board beamforming, and denote by $\mathbf{B}$ the corresponding $N \times K$ beamforming matrix. Assuming a perfectly calibrated and noiseless feeder link, linear precoding can be implemented on the beam signals at the GW, such that

$$\mathbf{x} = \mathbf{B}\mathbf{F}_b \mathbf{s} \tag{5}$$

where $\mathbf{F}_b$ is the $K \times K$ precoder in the beam space, and the $K \times 1$ vector $\mathbf{s}$ is the stack of the information bearing constellation symbols of all UTs, with $\mathbf{E}\{\mathbf{s}\mathbf{s}^H\} = \mathbf{I}$.

(ii) Joint precoding and beamforming: without on-board beamforming, all feed signals are ideally assumed to be available on-ground, such that the precoding can be considered in the feed signal space:

$$\mathbf{x} = \mathbf{F}_f \mathbf{s} \tag{6}$$

with $\mathbf{F}_f$ the $N \times K$ precoder in the feed space. Comparing (5) and (6), we see that $\mathbf{F}_f$ is to be compared to $\mathbf{B}\mathbf{F}_b$. That is, precoding the feed space is equivalent to a joint beamforming and precoding design. Moreover, since $\mathbf{F}_f$ is of greater size than $\mathbf{F}_b$, it is obvious that considering the beamforming and precoding jointly cannot perform worse than considering them separately. Determining whether the joint design generates a substantial gain is the objective of this work.

Among all possible versions of linear precoders, we identified that the regularized channel inversion [6] achieves the best trade-off between performance and complexity, providing robustness to imperfect CSI at the GW. Defining $\mathbf{H}_b \doteq \mathbf{H}\mathbf{B}$, the corresponding expressions are

$$\mathbf{F}_b = \sqrt{\gamma_b}\, \hat{\mathbf{H}}_b^H \left(\hat{\mathbf{H}}_b \hat{\mathbf{H}}_b^H + \frac{K}{P}\mathbf{I} \right)^{-1} \tag{7}$$

$$\mathbf{F}_f = \sqrt{\gamma_f}\, \hat{\mathbf{H}}^H \left(\hat{\mathbf{H}} \hat{\mathbf{H}}^H + \frac{K}{P}\mathbf{I} \right)^{-1} \tag{8}$$

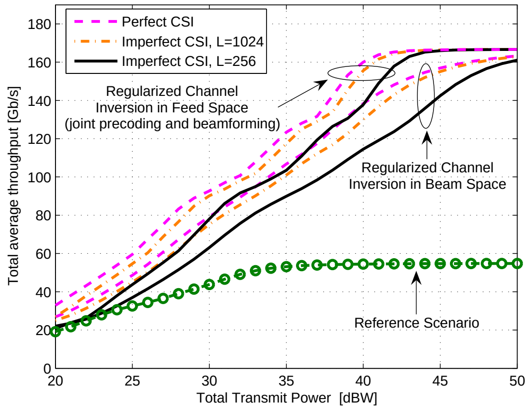

Fig. 4. Regularized channel inversion: evolution of throughput as a function of the total transmit power, and degree of CSI.

for the precoding in the beam space and feed space, respectively. The matrices $\hat{\mathbf{H}}_b$ and $\hat{\mathbf{H}}$ refer to the non-perfect channel estimates available at the GW. The values of the constants γ_b and γ_f have to be such as to comply with the above-mentioned transmit power constraint.

B. Simulation Results

The simulation results are related to a user link operating at 20 GHz (K_a band) on a 500 MHz total bandwidth divided into 12 carriers. As mentioned in Section III, the beam radiation pattern and the fixed beamforming $\mathbf{B}$ correspond to an European coverage with $N = 155$ and $K = 100$. FL performance has been evaluated by considering the working points (i.e. the required SINR) of the different modulation and coding modes of the DVB-S2 standard. As explained in Section III, the channel estimation is based on L-length orthogonal training sequences (WH codes). The rest of the simulation parameters are summarized in Table I.

Fig. 4 depicts the evolution of throughput of the proposed scheme as a function of the total transmit power, averaged on a thousand realizations of the rain fading and UTs locations. It also includes a reference scenario defined by (i) on-board fixed beamforming, (ii) no precoding on-ground, and (iii) a 3 colors frequency reuse pattern. The throughput gain generated by the joint precoding and beamforming is significant with respect to the reference scenario, and more limited (but not negligible) when compared to precoding in the beam space. At a total transmit power of 30 dBW and with perfect CSI, the proposed joint design generates a 111% throughput increase with respect to the reference scenario and a 17% increase when the processing is held in the beam space. The robustness to imperfect CSI is also illustrated. Quite interestingly, the gain of the joint design with respect to processing in the beam space increases as the degree of channel knowledge decreases: 20% for $L = 1014$ and 23% for $L = 256$ (at 30 dBW total transmit power again).

V. Multi-User Interference Mitigation for the Return Link

A. MUD Techniques for the Return Link

Comparison of linear and nonlinear MUD schemes has been performed, for both fixed beamforming and feed processing. Next we detail the employed MUD techniques, being $\hat{\mathbf{H}}$ and $\hat{\mathbf{H}}_b$ the non-perfect channel estimates of $\mathbf{H}$ and $\mathbf{H}_b \doteq \mathbf{BH}$ respectively, obtained as detailed earlier, where $\mathbf{B}$ denotes the on-board fixed beamforming.

1) Linear detection: The well-known MMSE combiner [7] was considered, so that, for the on-ground feed processing $\hat{\mathbf{x}} = \mathbf{W}_f^H \mathbf{y}$, with

$$\mathbf{W}_f^H = \left(N_0 \mathbf{I} + \hat{\mathbf{H}}^H \hat{\mathbf{H}}\right)^{-1} \hat{\mathbf{H}}^H \tag{9}$$

whereas the processing of the beams would entail $\hat{\mathbf{x}} = \mathbf{W}_b^H \mathbf{B} \mathbf{y}$ with

$$\mathbf{W}_b^H = \left(\mathbf{I} + \hat{\mathbf{H}}_b^H \boldsymbol{\Sigma}^{-1} \hat{\mathbf{H}}_b\right)^{-1} \hat{\mathbf{H}}_b^H \boldsymbol{\Sigma}^{-1} \tag{10}$$

where $\boldsymbol{\Sigma} \doteq \mathbf{E}\{\mathbf{Bn}(\mathbf{Bn})^H\}$, and N_0 denotes the noise power spectral density.

2) SIC detection: In this case, users are successively decoded following a given order. In terms of capacity, the sum-rate is the same regardless of the order, although the actual throughput changes with the ordering. For all simulations, a decreasing SINR order has been applied. The algorithm used is as follows: at each step, LMMSE combining is performed, the user with the best SINR is chosen and his contribution is subtracted from the overall signal. Then, the process is repeated on the remaining users, and so on until all of them have been extracted.

3) Performance effect of the jitter floor: When correlation is used to estimate the channel, an upper bound on the maximum SINR achievable after MUD appears. For the case of linear detection, this bound may be analytically obtained. Let $\mathbf{R} = \left(\mathbf{CC}^H\right)/L$ and consider the asymptotic case for which the noise power may be neglected, then the SINR for the i-th user can be shown to be

$$\mathrm{SINR}_i = \frac{1}{\left[\mathbf{R}^{-2} - 2\mathbf{R}^{-1} + \mathbf{I}\right]_{ii}}. \tag{11}$$

It can be noticed that under perfectly uncorrelated training sequences, $\mathbf{R} = \mathbf{I}$ and, in consequence, the upper bound would be $+\infty$.

B. Simulation Results

In order to assess the performance of the proposed MUD techniques, Monte Carlo simulations have been carried out according to the scenario described in Table I. Results have been averaged for a total of 1,000 realizations.

Fig. 5 depicts the evolution of the total throughput, scaled by the system's availability, as a function of the terminals EIRP. A significant improvement with respect to the reference scenario is observed: the scaled througput is almost doubled with non-perfect CSI and almost three times larger with perfect

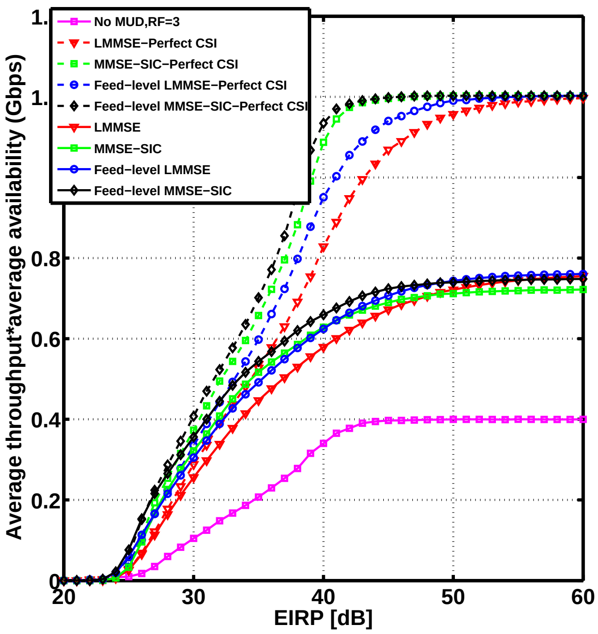

Fig. 5. Evolution of throughput as a function of the UT EIRP.

CSI. To this extent, asymptotic simulation results can be seen to be limited by an upper bound, as stated above. However, reasonable losses ocurr below 40 dBW, though at the expense of a rather high training sequence length.

Also, results show that feed-level techniques outperform those based on beam signals. Nevertheless, working with the 155 feed signals would require rather more bandwidth in the feeder link. Therefore, there exists a trade-off between performance and feeder link requirements, and the election of the most suitable MUD technique would need to take into account all these facts.

VI. Digital Feeder Link

Conventional beamforming techniques that uniquely rely on the payload's processing capabilities are nowadays far beyond the state of the art [9], while in case of full on ground beamforming the satellite must transfer to the ground segment all the signals received by each feed of its array fed reflector antenna. An alternative hybrid processing strategy is desirable, to reduce the number of signals to be relayed on ground while guaranteeing full flexibility to on ground signal processing. This implies the presence of an on-board fixed (i.e. non adaptive) compression scheme for reducing the amount of required spectral resources on the feeder link. In this work, we are inspired by the hybrid architecture described in [9]: the idea that justifies this approach is that, since feed radiation patterns overlap in space, feed signals present some degree of correlation. As a consequence, if projected on different domains through appropriate transforms, the number of relevant coefficients that carry most of the signal information reduces. We consider the return link of this satellite system and we assume that users are randomly positioned within each beam. At a generic time instant the feed signals $\mathbf{x}$ are down-converted, sampled and quantized before compression. We considered uniform quantization of the real part and the imaginary part of each of the elements of $\mathbf{x}$, yielding $\mathbf{x}_q$. Quantized feed signals are then sent through the compression stage, where they are projected on the space defined by matrix $\mathbf{V}$, yielding a new $N \times 1$ vector of coefficients $\bar{\mathbf{x}}$, that represent the feed signals in the new considered space. This vector is quantized again yielding to $\bar{\mathbf{x}}_q$ We will call the elements of $\bar{\mathbf{x}}$ feedlets. Thus, the following equation holds:

$$\bar{\mathbf{x}}_q = \mathcal{Q}\left(\mathbf{V}\mathcal{Q}\left(\mathbf{x}\right)\right) = \mathcal{Q}\left(\mathbf{V}\mathbf{x}_q\right). \tag{12}$$

Now compression is implemented, in the sense that the less relevant coefficients, in terms of magnitude, are discarded from $\bar{\mathbf{x}}_q$ yielding an $M \times 1$ vector $\bar{\mathbf{x}}_{M,q}$, with $M < N$, which is the compressed version of $\bar{\mathbf{x}}_q$. The M feedlets resulting from the compression stage are then multiplexed in frequency and polarization, and transmitted to the gateway on the feeder link. Assuming the feeder link is ideal, feedlets are processed through the inverse transformation, to extract the user signals through beamforming and Multi-User Detection techniques. We examine two different compression techniques, based on Discrete Fourier Transform (DFT), and Karhunen-Loeve Transform (KLT), respectively. From a practical point of view, this means that the matrix $\mathbf{V}$ in the first case is given by the DFT matrix, while in the second case it is given by the eigenvectors of the mean covariance channel matrix of the received signals. In order to assess performance, we used a figure of merit called Signal to Distortion Noise Ratio (SDNR), which measures the distortion between the vector of feed signals $\mathbf{x}$ and the vector of reconstructed feed signals $\hat{\mathbf{x}}$, obtained by applying the inverse of the considered transform to $\bar{\mathbf{x}}_{M,q}$. Clearly SDNR is a function of M and of the number of quantization levels, and we define it as:

$$\mathrm{SDNR} = \frac{< |\mathbf{x}|^2 >}{< |\mathbf{x} - \hat{\mathbf{x}}|^2 >}. \tag{13}$$

Fig. 6 shows the performance, in terms of SDNR in dB, for the two techniques, as the number of discarded coefficients $N - M$ varies. This is obviously related to the amount of bandwidth reduction, that can be quantified as $\frac{N-M}{N}$, since signals must be frequency-multiplexed. It can be seen how, with a 13% bandwidth reduction, different techniques perform quite differently, also as the number of quantization levels varies: the KLT transform yields SDNR $= 30$ dB, and SDNR $= 10$ dB for, respectively 2^{16} and 2^4 quantization levels, whereas DFT offers SDNR $= 20$ dB, and SDNR $= 10$ dB for the same quantization strategies. Clearly, the KLT shows better performance than the DFT being better "matched" to the incoming signal although it requires a calibration stage (i.e. the computation of the covariance matrix), while the advantage of DFT lies in its simplicity of implementation.

VII. Conclusions

In this paper we presented the advantages given by a hybrid space-ground processing architecture for broadband

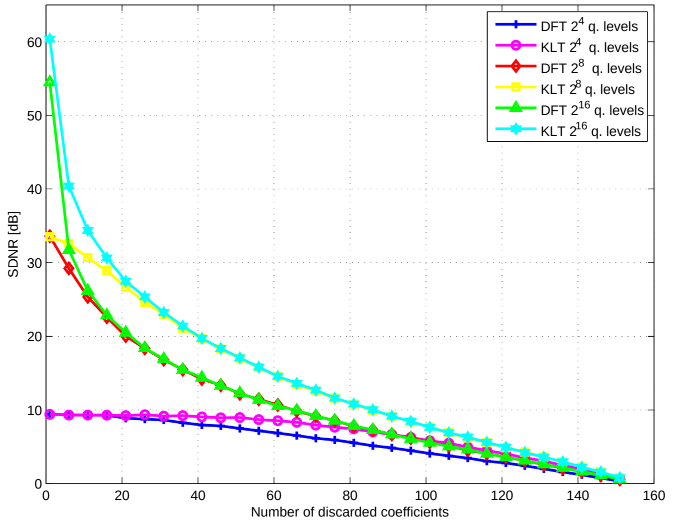

Fig. 6. DFT vs KLT, Freq. Reuse 1, EIRP = 60dBW

satellite communications. We discussed the issues related to channel estimation for a multi-beam system, identifying the most suitable solution for both forward and return link. Multi-user techniques have been introduced, namely precoding in the forward link and multi-user detection in the return link, and their effectiveness is discussed for a ideal CSI case and a more realistic case of non-ideal channel estimation. Finally the digitization of the feeder link has been considered, showing that feeder link bandwidth can be reduced without significantly affecting the signal quality. Summarizing, this paper is a first step towards the study and the realization of a hybrid space-ground processing system, which represents the optimum compromise between payload complexity, processing capabilities and bandwidth requirements.

Acknowledgment

This work has been partly supported by ESA contract 23089/10/NL/CLP "SatNEx Network of Experts"

References

[1] N. Zorba, M. Realp, A.I. Pérez-Neira, "An improved partial CSIT random beamforming for multibeam satellite systems",in Proc. 10th Int. Work. Signal. Process. Space Commun. (SPSC), Rhodes Island, Greece, Oct. 2008.

[2] G. Gallinaro, "Novel Intra-System Interference Mitigation Techniques and Technologies for Next Generations Broadband Satellite Systems", Final report of ESA/ESTEC contract No. 18070/04/NL/US.

[3] G. Caire, M. Debbah, L. Cottatellucci, R. De Gaudenzi, R. Rinaldo, R. Mueller, and G. Gallinaro, "Perspectives of Adopting Interference Mitigation Techniques in the Context of Broadband Multimedia Satellite Systems", in Proc. 23rd AIAA, Rome, Italy, Sept. 2005, pp. 1-5.

[4] L. Cottatellucci, M. Debbah, G. Gallinaro, R. Mueller, M. Neri, and R. Rinaldo, "Interference Mitigation Techniques for Broadband Satellite Systems", in Proc. 24th AIAA, San Diego, CA, June 2006, pp. 1-13.

[5] M. Bergmann, W. Gappmair, C. Mosquera, and O. Koudelka, "Channel Estimation on the Forward Link of Multi-Beam Satellite Systems", in Proc. 3rd Int. ICST Conf. Personal Satellite Services (PSATS), Malaga, Spain, Feb. 2011, pp. 250-259.

[6] C. B. Peel, B. M. Hochwald, and A. L. Swindlehurst, "A vector-perturbation technique for near capacity multiantenna multiuser communication-Part I: Channel inversion and regularization", IEEE Trans. on Communications, vol. 53, no. 1, pp.195-202, Jan. 2005.

[7] A. Paulraj, R. Nabar and D. Gore. "Introduction to Space-Time Wireless Communications", Cambridge University Press, 2003.

[8] P. Angeletti, G. Gallinaro, M. Lisi, and A. Vernucci, "On-ground digital beamforming techniques for satellite smart antennas", in Proc. 19th AIAA, Toulouse, France, April 2001, pp. 1-8.

[9] P. Angeletti and N. Alagha, "Space/Ground Beamforming Techniques for Emerging Hybrid Satellite Terrestrial Networks" , in Proc. 27th AIAA, Edinburgh, UK, June 2009, pp. 1-6.

[10] H. L. Van Trees, "Detection, Estimation, and Modulation Theory, Part IV: Optimum Array Processing", Wiley, 2002.